

Electron Delocalization in a Ruthenium(II) Bis(2,2':6',2''-terpyridyl) Complex

Andrew C. Benniston, Glen Chapman, Anthony Harriman,* Maryam Mehrabi, and Craig A. Sams

Molecular Photonics Laboratory, School of Natural Sciences (Chemistry), University of Newcastle, Newcastle upon Tyne, NE1 7RU United Kingdom

Received November 30, 2003

Photophysical properties have been recorded for a ruthenium(II) bis(2,2':6',2''-terpyridine) complex bearing a single ethynylene substituent. The target compound is weakly emissive in fluid solution at room temperature, but both the emission yield and lifetime increase dramatically as the temperature is lowered. As found for the unsubstituted parent complex, the full temperature dependence indicates that the lowest-energy triplet state couples to two higher-energy triplets and to the ground state. Luminescence occurs only from the lowest-energy triplet state, but the radiative and nonradiative decay rates indicate that electron delocalization occurs at the triplet level. Comparison of the target compound with the parent complex indicates that the ethynylene group reduces the size of the electron-vibrational coupling element for nonradiative decay of the lowest-energy triplet state. Although other factors are affected by substitution, this is by far the most important feature with regard to stabilization of the triplet state.

Introduction

It is well established that 2,2':6',2''-terpyridine (terpy) provides an ideal building block with which to assemble multicomponent molecular systems around photoactive transition metal centers.¹ The main advantages of the terpy module are its facile functionalization,² the ability to construct linear arrays,³ and the achiral nature of the resultant metal complexes. A major drawback, however, concerns the very short ($\tau < 1$ ns) triplet state lifetime found for the parent ruthenium(II) complex, $[\text{Ru}(\text{terpy})_2]^{2+}$, at ambient temperature.⁴ This short triplet lifetime, which precludes luminescence in fluid solution, is caused by coupling between the lowest-energy triplet state and a higher-energy metal-centered

(MC) state.⁵ Numerous attempts have been made to prolong the triplet lifetime of the parent complex. These include incorporating the chromophore into a zeolite structure⁶ and raising the energy of the metal-centered state by replacement of one terpy with three cyanide ligands.⁷ Other approaches have involved substituting electron-withdrawing groups at the 4'-position of the terpy ligand. This latter procedure has met with modest success, and triplet lifetimes as long as 10 ns have been reported.⁸

*To whom correspondence should be addressed. E-mail: anthony.harriman@ncl.ac.uk

- (1) (a) Sauvage, J.-P.; Collin, J.-P.; Chambron, J.-C.; Guillerez, S.; Coudret, C.; Balzani, V.; Barigelletti, F.; De Cola, L.; Flamigni, L. *Chem. Rev.* **1994**, *94*, 993. (b) Johansson, O.; Borgstrom, M.; Lomoth, R.; Palmblad, M.; Bergquist, J.; Hammarstrom, L.; Sun, L. C.; Akermark, B. *Inorg. Chem.* **2003**, *42*, 2908. (c) Constable, E. C.; Handel, R. W.; Housecroft, C. E.; Morales, A. F.; Flamigni, L.; Barigelletti, F. *J. Chem. Soc., Dalton Trans.* **2003**, 1220. (d) Yutaka, T.; Mori, I.; Kurihara, M.; Mizutani, J.; Tamai, N.; Kawai, N.; Irie, M.; Nishihara, H. *Inorg. Chem.* **2002**, *41*, 7143. (e) McMillin, D. R.; Moore, J. J. *Coord. Chem. Rev.* **2002**, *229*, 113.
- (2) (a) Heller, M.; Shubert, U. S. *Eur. J. Org. Chem.* **2003**, 947. (b) Andres, P. R.; Lunkwitz, R.; Pabst, G. R.; Böhn, K.; Wouters, D.; Schmatloch, S.; Shubert, U. S. *Eur. J. Org. Chem.* **2003**, 3769. (c) Harriman, A.; Hissler, M.; Khatyr, A.; Ziessel, R. *Eur. J. Inorg. Chem.* **2003**, 955. (d) Fallahpour, R. A. *Synthesis* **2003**, 155. (e) Heller, M.; Shubert, U. S. *Synlett* **2002**, 751.

- (3) (a) Collin, J.-P.; Gaviña, P.; Heitz, V.; Sauvage, J.-P. *Eur. J. Inorg. Chem.* **1998**, *1*, 1. (b) Haider, J. M.; Chavarot, M.; Weidner, S.; Sadler, I.; Williams, R. M.; De Cola, L.; Pikramenou, Z. *Inorg. Chem.* **2001**, *40*, 3912. (c) Flamigni, L.; Barigelletti, F.; Armardi, N.; Ventura, B.; Collin, J.-P.; Sauvage, J.-P. *Inorg. Chem.* **1999**, *38*, 661. (d) Flamigni, L.; Marconi, G.; Dixon, I. M.; Collin, J.-P.; Sauvage, J.-P. *J. Phys. Chem. B* **2002**, *106*, 6663. (e) Chichak, K.; Branda, N. R. *Chem. Commun.* **1999**, 523. (f) Flamigni, L.; Barigelletti, F.; Armaroli, N.; Collin, J.-P.; Sauvage, J.-P.; Williams, J. A. G. *Chem.—Eur. J.* **1998**, *4*, 1744. (g) Akasaka, Y.; Mutai, T.; Otsuki, J.; Araki, K. *J. Chem. Soc., Dalton Trans.* **2003**, 1537. (h) Gohy, J. F.; Lohmeijer, B. G. G.; Shubert, U. S. *Chem.—Eur. J.* **2003**, *9*, 3472. (i) Wang, X. Y.; Del Guercio, A.; Schmehl, R. H. *Chem. Commun.* **2002**, 2344. (j) Harriman, A.; Mayeux, A.; De Nicola, A.; Ziessel, R. *Phys. Chem. Chem. Phys.* **2002**, *4*, 2229.
- (4) Winkler, J. R.; Netzel, T. L.; Creutz, C.; Sutin, N. *J. Am. Chem. Soc.* **1987**, *109*, 2381.
- (5) (a) Coe, B. J.; Thompson, B. W.; Culbertson, C. D.; Shoonover, J. R.; Meyer, T. J. *Inorg. Chem.* **1995**, *34*, 3385. (b) Clark, R. H.; Ann, K. I. G.; David, R. M. *Inorg. Chem.* **1991**, *30*, 538. (c) Kirchoff, J. R.; McMillin, D. R.; Marnot, P. A.; Sauvage J.-P. *J. Am. Chem. Soc.* **1985**, *107*, 1138.
- (6) Bhuiyan, A. A.; Kincaid, J. R. *Inorg. Chem.* **1998**, *37*, 2525.
- (7) Indelli, M. T.; Bignozzi, C. A.; Scandola, F.; Collin, J.-P. *Inorg. Chem.* **1998**, *37*, 6084.

A related strategy for prolonging the triplet lifetime has focused on attaching alkynylene groups at the 4'-position.⁹ The acetylenic residue raises the reduction potential for the coordinated terpy ligand to a less negative value.¹⁰ Because the oxidation potential for the metal cation is essentially unaffected by this substitution, the net effect is to lower the energy of the metal-to-ligand charge-transfer (MLCT) triplet state. In turn, this effect helps to decouple the MLCT triplet from higher-energy MC states and thereby prolongs the triplet lifetime.¹¹ Because of the extended π -conjugation over the substituted ligand, there is increased opportunity for electron delocalization at the triplet level. Such delocalization should lower the nuclear reorganization energy that accompanies nonradiative decay of the MLCT triplet by providing additional degenerate vibrational modes to accommodate any geometric change.¹² Within the framework of the Englman–Jortner energy-gap law,¹³ this will further stabilize the triplet state. The overall result is nontrivial, and triplet lifetimes of 55 and 565 ns, respectively, have been reported for the ethynylene-substituted mono- and binuclear complexes at room temperature.¹⁴ Extending the conjugation with a bridging butadiynylene group extends the triplet lifetime of the resultant binuclear complex to 720 ns.⁹

Thus, the presence of an alkynylene group at the 4'-position of the terpy ligand is expected to stabilize the triplet lifetime of the corresponding ruthenium(II) complex. Although there is considerable literature information¹⁵ to support this notion, the detailed mechanism by which the triplet lifetime is prolonged has not been clarified. In particular, and in contrast to the analogous 2,2'-bipyridine complexes,¹⁶ the importance of electron delocalization at the triplet level has not been elucidated. Here, we examine the effect of temperature on the luminescence yield and lifetime recorded for a ruthenium(II) bis(2,2':6',2''-terpyridine) complex bearing a single ethynylene substituent at the 4'-position (Figure 1). The objective is to compare the photophysical properties with those of the parent complex, $[\text{Ru}(\text{terpy})_2]^{2+}$, in an effort to distinguish between decoupling of MC and MLCT triplet states and electron delocalization at the triplet level. A further motivation for this work is to provide photophysical data for the ruthenium(II)-based terminal of photoactive dyads and triads displaying intramolecular triplet energy transfer.¹⁷ Related work by Meyer et al.¹⁸ has shown how the rates of radiative and nonradiative decay of selected osmium(II) poly-

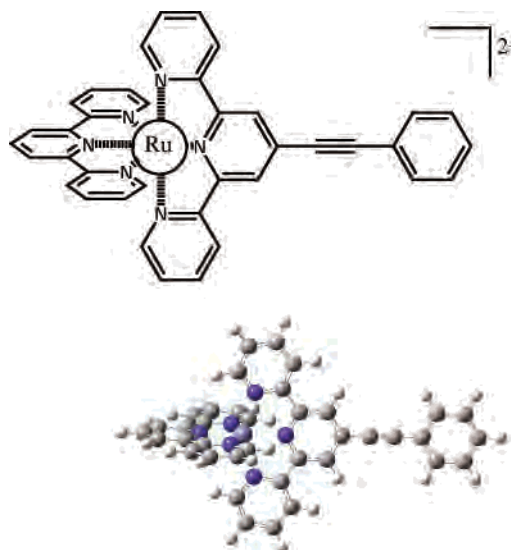


Figure 1. Molecular structure and energy-minimized conformation computed for **1**.

(pyridine) complexes can be calculated from absorption, emission, and resonance Raman spectra.

Experimental Section

All raw materials were purchased from Aldrich Chemicals Co. and were used as received. Solvents were dried by standard literature methods¹⁹ before being distilled and stored under nitrogen over 4 Å molecular sieves. ¹H and ¹³C NMR spectra were recorded with a JEOL Lambda 500 spectrometer. Routine mass spectra and elemental analyses were obtained using in-house facilities. The starting materials $[\text{Ru}(\text{terpy})(\text{CH}_3\text{CN})_3](\text{PF}_6)_2$ ²⁰ and trifluoromethane sulfonic acid [2,2':6',2''-terpyridin-4'-yl ester]²¹ were prepared and purified by literature methods.

Cyclic voltammetry experiments were performed using a fully automated HCH Instruments electrochemical analyzer and a three-electrode set-up consisting of a glassy carbon working electrode, a platinum wire counter electrode, and an SCE reference electrode. All experiments were performed in dry CH_3CN containing tetra-*N*-butylammonium tetrafluoroborate (0.2 mol dm^{-3}) as the background electrolyte. Absorption spectra were recorded with a Hitachi U3310 spectrophotometer, while corrected luminescence spectra were recorded with a Hitachi F4500 spectrophotometer. All luminescence measurements were made using optically dilute solutions and were corrected for spectral imperfections of the instrument by reference to a standard lamp. Emission quantum yields were measured relative to ruthenium(II) tris(2,2'-bipyridine).²² Time-resolved luminescence measurements were made with a Spex Fluorolog Tau-3 spectrophotometer. Laser flash photolysis studies were made at the FRRF housed in the Daresbury Laboratory (United Kingdom). Excitation was made with a frequency-doubled, Q-switched

- (8) Constable, E. C.; Cargill Thompson, A. M. W.; Armaroli, N.; Balzani, V.; Maestri, M. *Polyhedron* **1992**, *11*, 2707.
 (9) Benniston, A. C.; Grossshenny, V.; Harriman, A.; Ziessel, R. *Angew. Chem., Int. Ed. Engl.* **1994**, *33*, 1884.
 (10) Harriman, A.; Hissler, M.; Ziessel, R. *Phys. Chem. Chem. Phys.* **1999**, *1*, 4203.
 (11) Harriman, A.; Khatyr, A.; Ziessel, R. *J. Chem. Soc., Dalton Trans.* **2003**, 2061.
 (12) Grossshenny, V.; Harriman, A.; Romero, F. M.; Ziessel, R. *J. Phys. Chem.* **1996**, *100*, 17472.
 (13) Englman, R.; Jortner, J. *Mol. Phys.* **1970**, *18*, 145.
 (14) Grossshenny, V.; Harriman, A.; Ziessel, R. *Angew. Chem., Int. Ed. Engl.* **1996**, *34*, 2705.
 (15) Harriman, A.; Ziessel, R. *Coord. Chem. Rev.*, **1998**, *171*, 331.
 (16) (a) Wang, Y. S.; Liu, S. X.; Pinto, M. R.; Dattlebaum, D. M.; Schoonover, J. R.; Schanze, K. S. *J. Phys. Chem. A* **2001**, *105*, 11118.
 (b) Forster, L. S. *Coord. Chem. Rev.* **2002**, *227*, 59. (c) Damrauer, N. H.; Weldon, B. T.; McCusker, J. K. *J. Phys. Chem. A* **1998**, *102*, 3382.

- (17) (a) Benniston, A. C.; Li, P.; Sams, C. A. *Tetrahedron Lett.* **2003**, *44*, 3947. (b) Benniston, A. C.; Harriman, A.; Li, P.; Sams, C. A. *Tetrahedron Lett.* **2003**, *44*, 4167.
 (18) Graff-Thompson, D.; Schoonover, J. R.; Timpson, C. J.; Meyer, T. J. *J. Phys. Chem. A* **2003**, *107*, 10250.
 (19) Perrin, D. D.; Armarego, W. L. F. *Purification of Laboratory Chemicals*, 3rd ed.; Pergamon Press Ltd.: Oxford, 1988.
 (20) Suen, H. F.; Wilson, S. W.; Pomerantz, M.; Walsh, J. L. *Inorg. Chem.* **1989**, *28*, 786.
 (21) Potts, K. T.; Konwar, D. *J. Org. Chem.* **1991**, *56*, 4815.
 (22) (a) Demas, J. N.; Crosby, G. A. *J. Am. Chem. Soc.* **1971**, *93*, 2741. (b) El-ghayoury, A.; Harriman, A.; Khatyr, A.; Ziessel, R. *J. Phys. Chem. A* **2000**, *104*, 1512.

Nd:YAG laser (fwhm = 10 ns, $\lambda = 532$ nm). The monitoring beam was provided with a pulsed, high-intensity Xe arc lamp.

Computational studies were made with the TITAN package²³ run on a fast PC. Several geometry optimizations were performed using the semiempirical PM3 method, starting from different initial geometries. All calculations were run in vacuo and in the absence of the counterions.

Synthesis of 4'-Phenylethynyl-[2,2':6',2'']terpyridine. A solution of trifluoromethane sulfonic acid [2,2':6',2'']terpyridin-4'-yl ester (1.00 g, 2.62 mmol), Pd(PPh₃)₄ (0.15 g, 0.13 mmol), and phenylacetylene (0.33 g, 3.23 mmol) in THF (22 mL) containing diisopropylamine (15 mL) was heated at 95 °C for 16 h under a dry dinitrogen atmosphere. The solution was allowed to cool to room temperature, followed by removal of the organic solvents under reduced pressure. The crude product was dissolved in dichloromethane (30 mL) and washed with distilled water (3 × 30 mL). The aqueous layer was separated and extracted with dichloromethane (2 × 20 mL). The combined organic layers were dried over MgSO₄, filtered, and evaporated under reduced pressure. The crude product was recrystallized from methanol to produce an off-white solid (0.65 g, 74%), mp = 144–146 °C. ¹H NMR (CDCl₃): δ 8.66–8.64 (2H, d, $J = 4$ Hz), 8.55 (2H, d, $J = 8$ Hz), 8.54 (2H, s), 7.83–7.76 (2H, dt, $J = 8$ Hz, $J' = 1.5$ Hz), 7.53–7.50 (2H, m), 7.33–7.26 (5H, m). ¹³C NMR (CDCl₃): δ 156.1, 155.9, 149.6, 137.3, 133.9, 132.4, 129.4, 128.9, 124.4, 123.2, 122.9, 121.6, 94.2, 87.9. EIMS calcd for MH⁺ 333.1269, found 333.1266. Elemental analysis calcd for C₂₃H₁₅N₃·H₂O: C 78.61, N 11.96, H 4.88%. Found: C 78.32, N 11.60, H 4.88%.

Synthesis of [Ru(4'-Phenylethynyl-[2,2':6',2'']terpyridine)(CH₃CN)₃](PF₆)₂. A solution of 4'-phenylethynyl-[2,2':6',2'']terpyridine (0.60 g, 1.80 mmol) and RuCl₃·xH₂O (0.41 g) in methanol (50 mL) was refluxed for 4 h under a dry dinitrogen atmosphere. The mixture was cooled to 0 °C in an ice bath and the resultant solid filtered and washed with methanol (50 mL) and diethyl ether (3 × 50 mL). The brown solid was dried under vacuum. This material (0.32 g, 0.59 mmol) was dissolved in a 1:1 methanol/acetonitrile mixture (25 mL) containing AgBF₄ (0.69 g, 3.54 mmol). The mixture was heated to reflux for 16 h under a dry dinitrogen atmosphere and in the absence of light. The solution was cooled to 0 °C in an ice bath and filtered to remove all silver complex impurities. An aqueous (1 M) KPF₆ solution was added slowly to the solution to precipitate the desired product. The solid was filtered and washed with distilled water (50 mL), methanol (50 mL), and diethyl ether (3 × 50 mL). It was air-dried for 5 min and vacuum-dried to produce the required compound as an orange powder (0.32 g, 21%), mp > 250 °C. ¹H NMR (CD₃CN): δ 8.97–8.95 (2H, d, $J = 6$ Hz), 8.56 (2H, s), 8.45 (2H, d, $J = 8$ Hz), 8.27–8.20 (2H, dt, $J = 8$ Hz, $J' = 1.5$ Hz), 7.82–7.80 (1H, dd, $J = 5$ Hz, $J' = 1$ Hz), 7.80–7.77 (1H, dd, $J = 5$ Hz, $J' = 1$ Hz), 7.77–7.73 (2H, m), 7.59–7.57 (2H, d, $J = 2$ Hz), 7.56 (1H, d, $J = 2$ Hz), 2.79 (3H, s), 2.19 (6H, s). ¹³C NMR (d₆-DMSO): δ 158.9, 158.0, 154.7, 138.8, 132.2, 131.4, 130.8, 129.6, 128.9, 128.8, 125.2, 125.1, 124.5, 120.9, 97.2, 86.7, 4.5, 3.5.

Synthesis of 1. A solution of [Ru(4'-phenylethynyl-[2,2':6',2'']terpyridine)(CH₃CN)₃](PF₆)₂ (0.36 g, 0.42 mmol) and 2,2':6',2'']terpyridine (0.10 g, 0.42 mmol) in a mixture of butanol (50 mL) and acetone (20 mL) was refluxed for 24 h under a dry dinitrogen atmosphere. The solution was cooled to room temperature, and the organic solvents were removed under reduced pressure. To the resultant residue was added dichloromethane (10 mL), and the insoluble solid was filtered and washed with dichloromethane (2

× 10 mL). After removal of the organic solvent, the residue was allowed to air-dry for 5 min and then dried under vacuum to afford the complex as a pinkish-red solid (0.16 g, 39%), mp > 250 °C. An analytically pure sample of **1** was obtained by slow vapor diffusion of diethyl ether into an acetonitrile solution containing the material. ¹H NMR (CD₃CN): δ 8.90 (2H, s), 8.84 (2H, d, $J = 8$ Hz), 8.55–8.49 (4H, t, $J = 8$ Hz), 8.49–8.43 (1H, t, $J = 8$ Hz), 8.00–7.92 (4H, 2 × ddd, $J = 8$ Hz, $J' = 5$ Hz, $J'' = 1.5$ Hz), 7.84–7.80 (2H, m), 7.61–7.60 (3H, m), 7.43–7.38 (4H, 2 × dd, $J = 5$ Hz, $J' = 1.5$ Hz), and 7.24–7.17 (4H, 2 × ddd, $J = 8$ Hz, $J' = 5$ Hz, $J'' = 1.5$ Hz). ¹³C NMR (CD₃CN): δ 157.6, 157.1, 155.1, 154.9, 152.3, 152.2, 137.9, 137.8, 135.8, 131.8, 130.0, 129.7, 128.8, 127.4, 127.1, 124.9, 124.2, 124.2, 123.5, 121.0, 96.4, 85.9. Elemental analysis calcd for **1**, CH₃CN(3H₂O)-C₄₀H₃₅N₇RuP₂F₁₂O₂: C 45.64, H 3.35, N 9.31%. Found: C 45.14, H 3.00, N 9.58%. Electrospray-MS m/z calcd for [M - PF₆]⁺ = 813.1, found 812.9; m/z calcd for [M - 2PF₆]²⁺ = 334.1, found 334.0.

Results and Discussion

The mononuclear complex **1** was readily prepared in three steps by first reacting RuCl₃·xH₂O with 1 equiv of 4'-phenylethynyl-[2,2':6',2'']terpyridine **L**, which itself was synthesized by a cross-coupling reaction between phenylacetylene and trifluoromethane sulfonic acid [2,2':6',2'']terpyridin-4'-yl ester. The resultant complex RuLCl₃ was converted to [Ru(L)(CH₃CN)₃](PF₆)₂ which, when reacted with 2,2':6',2'']terpyridine, afforded the desired complex. An analytically pure sample of **1** was prepared by multiple recrystallization from acetonitrile/diethyl ether. The compound, after isolation as the bis-hexafluorophosphate salt, was relatively soluble in most polar organic solvents at room temperature. It was stable toward prolonged storage in ambient light. Characterization was made on the basis of ¹H and ¹³C NMR spectroscopy, elemental analysis, and mass spectrometry. The energy-minimized structure is shown in Figure 1 and confirms the expected pseudo-octahedral geometry around the metal center. The phenylene ring appears to lie coplanar with the attached terpy ligand in an orientation that maximizes orbital overlap throughout the ligand. However, there is only a small barrier to rotation around the ethynylene bond.

Cyclic voltammetry showed that the metal center undergoes a quasireversible ($\Delta E_p = 70$ mV), one-electron oxidation process with a half-wave potential ($E_{1/2}$) of 1.33 V versus Ag/AgCl. Two successive quasireversible, one-electron reduction processes are found with $E_{1/2}$ values of -1.11 V ($\Delta E_p = 70$ mV) and -1.43 V versus Ag/AgCl ($\Delta E_p = 60$ mV), respectively. Comparison to related complexes^{9,10,15} indicates that the first reduction step corresponds to addition of an electron to the ethynylated terpyridine ligand. The second reductive process is due to electron attachment to the unsubstituted terpyridine. That this latter reduction is much easier than for the parent complex, [Ru(terpy)₂]²⁺ ($E_{1/2} = -1.25$ V and -1.52 V vs Ag/AgCl), is probably attributable to partial electron delocalization over the ethynylene group, reducing electrostatic factors. It is also clear that the large difference in $E_{1/2}$ values will localize the added electron at the substituted ligand. Oxidation of the metal center in **1** occurs at the same potential as for the parent complex.

(23) Wavefunction Inc.

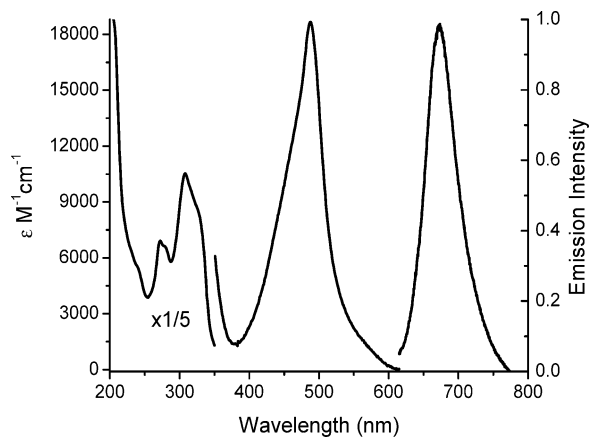


Figure 2. Absorption and emission spectra recorded for **1** in dilute butyronitrile solution at room temperature.

The absorption spectrum recorded for **1** in dilute butyronitrile solution exhibits an intense (formally) spin-allowed, metal-to-ligand charge-transfer (MLCT) transition centered at 490 nm (Figure 2). There is a fairly intense tail on the low-energy side that stretches as far as 620 nm and can be attributed to the spin-forbidden MLCT absorption transitions. On the higher energy side, the ethynylene-substituted terpyridine ligand absorbs between 300 and 350 nm, while the unsubstituted terpyridine ligand shows an absorption band at ca. 280 nm. The MLCT region is assumed to contain contributions arising from electron injection into both parent and substituted ligands. Weak phosphorescence can be detected in deoxygenated solution at room temperature (Figure 2). This emission peak is relatively narrow and is centered at 680 nm. The corrected excitation spectrum shows good agreement with the absorption spectrum, and the emission profile remains independent of excitation wavelength. In deoxygenated butyronitrile, the emission quantum yield (Φ_{LUM}) was found to be 0.00036 ± 0.00005 , and the emission lifetime (τ_{LUM}) was 44 ± 3 ns. Time-resolved emission decay profiles were strictly monoexponential at all monitoring wavelengths, but the derived lifetime was shortened by the presence of molecular oxygen. The emission yield and lifetime are comparable to those reported earlier for a somewhat related mononuclear complex,⁹ and in particular, the lifetime is significantly longer than that of the parent.⁴

Laser flash photolysis studies, with excitation at 532 nm, gave access to the lowest-energy MLCT triplet state. This species, which retains the same lifetime as that recorded from time-resolved emission spectroscopy, displays the transient differential absorption spectrum shown in Figure 3. There is strong bleaching of the spin-allowed MLCT band at 490 nm and weaker absorption stretching toward both higher and lower energies. Absorption reaches out as far as 800 nm. The derived differential absorption spectrum is similar to spectra recorded for related ethynylated Ru-terpy derivatives.^{2c,12,22b,24} Decay kinetics were independent of monitoring wavelength and laser intensity. The similarity in lifetimes derived by the two techniques confirms that the observed emission is from the lowest-energy MLCT triplet state.

It was noted that the emission quantum yield and lifetime increased progressively with decreasing temperature

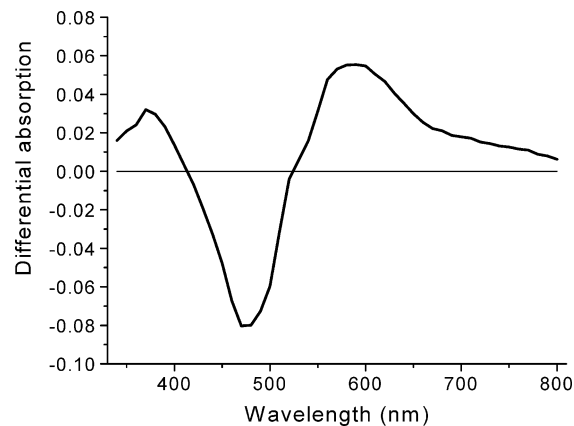


Figure 3. Differential transient absorption spectrum recorded 20 ns after laser excitation of **1** in deoxygenated acetonitrile at room temperature.

(Figure 4). There was no obvious spectral shift upon cooling. At the lowest temperature studied ($T = 80$ K), where the solvent is frozen, Φ_{LUM} is increased to 0.225 while τ_{LUM} is 27.4 μs . At intermediate temperatures, the nonradiative decay rate constant [$k_{\text{D}} = (1 - \Phi_{\text{LUM}})/\tau_{\text{LUM}}$] was found to follow an Arrhenius-type expression that involves a 4-state model (Figure 5).²⁵ Here, the lowest-energy MLCT triplet is coupled to the ground state and to two higher-lying triplet states. Access to the first of these triplets involves crossing a barrier (E_{A}) of only 835 cm^{-1} , but reaching the higher-lying triplet involves overcoming a more substantial barrier ($E_{\text{B}} = 2675$ cm^{-1}). Following from earlier work,^{5,25,26} it is assumed that the uppermost triplet state is an MC state that is strongly coupled to the ground state. There is no direct spectroscopic evidence for this assignment, but it remains the most reasonable possibility. The other triplet state is assumed to be an additional MLCT triplet but with more singlet character.²⁷ At low temperature, nonradiative decay of the lowest-energy MLCT triplet is activationless and occurs with a rate constant (k_0) of 3.2×10^4 s^{-1} . This latter value is close to the radiative rate constant ($k_{\text{RAD}} = 8 \times 10^3$ s^{-1}).

$$k_{\text{D}} = \frac{(k_0 + k_1 \exp^{-E_{\text{A}}/k_{\text{B}}T} + k_{\text{P}} \exp^{-E_{\text{B}}/k_{\text{B}}T})}{1 + \exp^{-E_{\text{A}}/k_{\text{B}}T}} \quad (1)$$

In fitting the experimental data, it was necessary to include two activated processes and an activationless decay route.^{25,28,29} Even so, several models are possible, and we have opted to use the model developed by Demas et al.³⁰ Here, both MLCT triplets are coupled to the uppermost MC triplet by way of activated processes (Figure 5). The energies of these MLCT

(24) El-ghayoury, A.; Harriman, A.; Ziessel, R. *J. Phys. Chem. A* **2000**, *104*, 7906.

(25) (a) Allsopp, S. R.; Cox, A.; Jenkins, S. H.; Kemp, T. J.; Tunstall, S. M. *Chem. Phys. Lett.* **1976**, *43*, 135. (b) Hecker, C. R.; Gushurst, A. K. I.; McMillan, D. R. *Inorg. Chem.* **1991**, *30*, 538.

(26) Amini, A.; Harriman, A.; Mayeux, A. *Phys. Chem. Chem. Phys.* **2004**, *6*, 1157.

(27) Kober, E. M.; Meyer, T. J. *Inorg. Chem.* **1984**, *23*, 3877.

(28) Harrigan, R. W.; Hager, G. D.; Crosby, G. A. *Chem. Phys. Lett.* **1973**, *21*, 487.

(29) (a) Maruszewski, K.; Kincaid, J. R. *Inorg. Chem.* **1995**, *34*, 2002. (b) Sykora, M.; Kincaid, J. R. *Inorg. Chem.* **1995**, *34*, 5852.

(30) Sacksteder, L. A.; Lee, M.; Demas, J. N.; DeGraff, B. A. *J. Am. Chem. Soc.* **1993**, *115*, 8230.

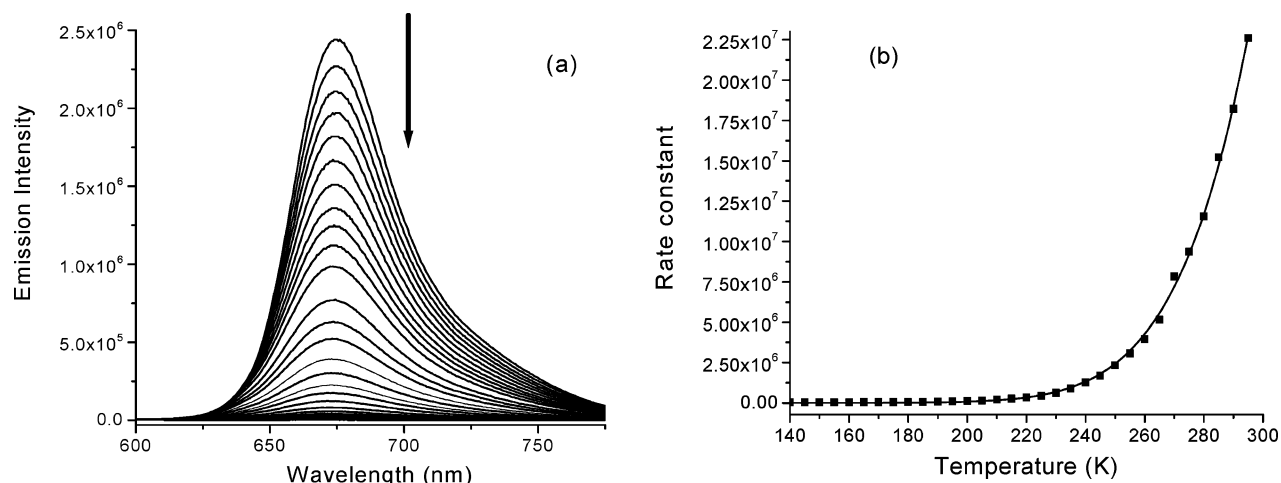


Figure 4. (a) Effect of temperature on the emission spectral profile recorded for **1** in butyronitrile. (b) Fit of the measured rate constant for nonradiative decay to eq 1 with the parameters collected in Table 1.

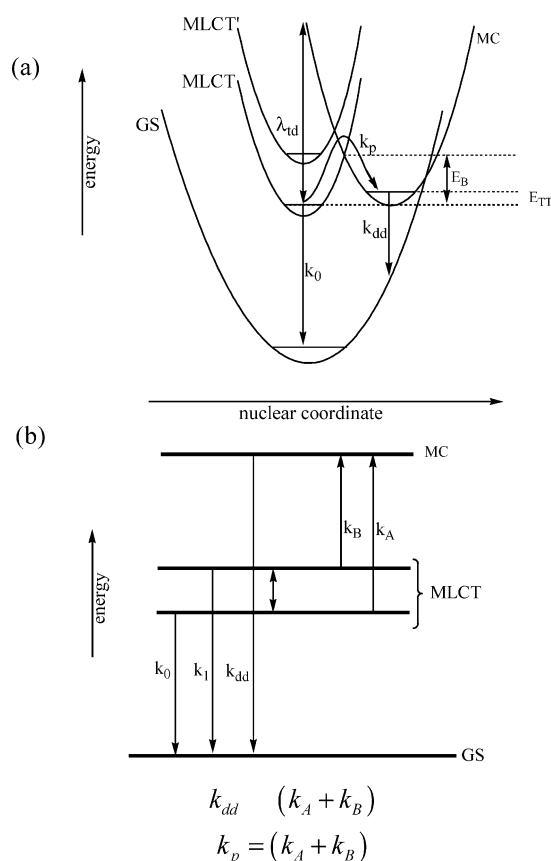


Figure 5. Energy level diagram proposed for the triplet manifold of **1**. Interconversion between the lowest-energy MLCT triplet state (MLCT) and the second triplet (MLCT') is assumed to be reversible, but population of the metal-centered triplet state (MC) is followed by rapid decay to the ground state. Note that in the potential energy diagram (a) the position of the second MLCT triplet has been displaced to higher energy for clarity of presentation.

triplets are sufficiently close for the two states to lie in thermal equilibrium at reasonable temperatures, and it is assumed that both states undergo nonradiative decay to the ground state. Within this model, the nonradiative decay rate constants for deactivation of the lowest-energy MLCT state, the upper-lying MLCT triplet, and the MC state are designated as k_0 , k_1 , and k_{dd} , respectively. Internal conversion from the MC state is likely to be very fast³⁰ such that, once

Table 1. Comparison of the Derived Parameters Controlling Deactivation of the Lowest-Energy Triplet Excited States of **1** and $[\text{Ru}(\text{terpy})_2]^{2+}$ in Deoxygenated Butyronitrile

property	1	$[\text{Ru}(\text{terpy})_2]^{2+}$
E_0/cm^{-1}	14 860	16 230
E_T/cm^{-1}	15 540	16 950
$h\nu/\text{cm}^{-1}$	1 300	1 370
λ_T/cm^{-1}	680	720
S	0.62	0.68
k_0/s^{-1}	3.2×10^4	6.5×10^4
k_1/s^{-1}	5.0×10^7	2.1×10^7
E_A/cm^{-1}	835	720
k_p/s^{-1}	1.6×10^{13}	2.0×10^{13}
E_B/cm^{-1}	2 675	1 700
k_{RAD}/s^{-1}	8×10^3	4×10^4
$M/\text{\AA}$	0.038	0.023
C/cm^{-1}	1 300	2 640
g	1.91	1.86

populated, this state decays rapidly to the ground state. The rate constant for population of the MC state from each MLCT triplet is activated and follows an Arrhenius-type expression.

$$k_A = k_A^0 \exp^{-E_A/k_B T}$$

$$k_B = k_B^0 \exp^{-(E_B - E_A)/k_B T} \quad (2)$$

Given that the rate constants for formation of the MC state from the lowest- and higher-energy MLCT states, respectively, are k_A and k_B , it follows that

$$k_p = k_A^0 + k_B^0 \quad (3)$$

From the data analysis³⁰ (Table 1), it appears that k_1 is some 1000-fold faster than k_0 . This difference is attributed to the increased singlet-state character of the upper-lying MLCT triplet.²⁷ It is worth noting that the photophysical properties of the ruthenium(II) complex bearing two phenylethynylated terpyridine ligands remain identical to those recorded for **1**. This finding implies that the upper MLCT triplet state is not formed by charge injection into the parent ligand. The combined rate constant (k_p) for reaching the uppermost state is on the time scale expected for a vibration,³¹ but this process refers to an endoergic electron-transfer step.³² As such, the activation energy (E_B) comprises terms

associated with the reorganization energy (λ_{id}) and the spectroscopic energy gap (E_{TT}) between the MLCT and MC states. None of these terms are available for **1**. Presumably, k_{A} and k_{B} are of comparable magnitude. It should be noted that a prior investigation of the photophysical properties of the parent complex in the solid state considered that k_{dd} , rather than k_{p} , was the rate-determining step for the highly activated decay process.³³ This latter pathway was treated as an electron-transfer reaction, rather than as internal conversion via vibrational modes. Some support for this hypothesis can be derived from two-photon transient absorption spectroscopic studies³⁴ made with ruthenium(II) tris-(2,2'-bipyridine), where the lifetime of the MC state was reported to be some 270 ns. Our experimental results do not distinguish k_{dd} or k_{p} as being the rate-determining step, but the observation of a large activation energy (E_{B}) suggests that population of the MC state is slower than its subsequent decay (Figure 5).

The luminescence profile recorded over the temperature range 140–250 K, where the signal is relatively intense, could be analyzed³⁵ in terms of three Gaussian components of common half-width (fwhm = 1020 cm^{-1}). The highest-energy Gaussian component, which corresponds to the 0,0 transition, is centered at 14 860 cm^{-1} . From the half-width,³⁶ the total reorganization energy (λ_{T}) accompanying deactivation of the lowest-energy MLCT triplet is estimated to be ca. 680 cm^{-1} , while the weighted-average, medium-frequency vibrational mode ($h\omega_{\text{M}}$) coupled to nonradiative decay is calculated to be 1300 cm^{-1} . On this basis, the triplet energy (E_{T}) has a value of ca. 15 560 cm^{-1} . It should be noted that a low-frequency vibrational mode ($h\omega_{\text{L}}$ = 630 cm^{-1}) has to be included when the solute is present in a low-temperature glass.³⁷

The various parameters derived from the emission spectrum were refined by reconstituting the entire spectrum on the basis of a single averaged vibrational mode. In this procedure, the emission intensity, $I(\nu)$, at wavenumber ν relative to the intensity of the 0,0 transition is given by eq 4.³⁶ Here, m is the number of quanta of vibrational frequency $h\omega_{\text{M}}$ and displacement S . The term E_{00} refers to the energy of the 0,0 transition, and $\Delta\nu_{1/2}$ is the full-width at half-maximum of the individual vibronic components. The displacement S is also known as the Huang–Rhys factor.³⁸

Equation 4 gives a good representation of the emission spectrum recorded in fluid solution and with the parameters listed in Table 1. Refinement had little effect on either E_{00} or $\Delta\nu_{1/2}$ but allowed determination of S . Increasing the number of vibrational quanta beyond $m = 6$ had little, if any, effect on the quality of the fit.

$$\frac{I(\nu)}{I_{00}} = \sum_m \left[\left(\frac{E_{00} - m\hbar\omega_{\text{M}}}{E_{00}} \right)^3 \frac{S^m}{m!} \exp \left(-4 \ln 2 \left(\frac{\nu - E_{00} + m\hbar\omega_{\text{M}}}{\Delta\nu_{1/2}} \right)^2 \right) \right] \quad (4)$$

The radiative rate constant, k_{RAD} , can be expressed in terms of eq 5 where n is the refractive index of the solvent and M is the vibronic transition moment (Table 1).³⁹ The term $\langle \nu^{-3} \rangle$

$$k_{\text{RAD}} = \frac{32\pi^3 n^3}{3h} \left| \frac{e^2 M^2}{4\pi\epsilon_0} \right| \langle \nu^{-3} \rangle^{-1} \quad (5)$$

refers to the average emission energy (in units of cm^{-1}).⁴⁰ Evaluation of these expressions allows calculation of M as being 0.038 Å. This latter parameter can also be obtained by treating the emission spectrum in terms of the Franck–Condon factor,⁴¹ but this was not attempted here. Instead, the activationless rate constant for nonradiative decay, k_0 , was used to estimate the magnitude of the vibronically induced electronic coupling matrix element (C) according to¹³

$$k_{\text{NR}} = \frac{\sqrt{2\pi}C^2}{\hbar\sqrt{\hbar\omega_{\text{M}}E_{00}}} \exp(-S_{\text{M}}) \exp \left[\frac{\gamma E_{00}}{\hbar\omega_{\text{M}}} \right] \quad (6)$$

Here, the parameter γ depends not only on the amount of energy to be dissipated during nonradiative decay but also on the size of $h\omega_{\text{M}}$ and the magnitude of the reduced displacement of the accepting vibrational modes (Δ_{M}).⁴²

$$\gamma = \ln \left(\frac{E_{00}}{S_{\text{M}}\hbar\omega_{\text{M}}} \right) - 1 = \ln \left(\frac{2E_{00}}{d\Delta_{\text{M}}^2\hbar\omega_{\text{M}}} \right) - 1 \quad (7)$$

Evaluating eq 7 over the full temperature range allows the derivation of $\gamma = 1.91$ which, when used in conjunction with eq 6, results in an estimate for C of 1300 cm^{-1} .

It is instructive to compare these derived values with those reported earlier for the parent complex,²⁶ $[\text{Ru}(\text{terpy})_2]^{2+}$, under identical experimental conditions (Table 1). Thus, the triplet energy of **1** is reduced by ca. 1410 cm^{-1} , while the total reorganization energy is decreased slightly. The former observation is in accord with the measured reduction potentials, which suggest that the lowest-energy MLCT triplet is formed by charge injection from metal center to the ethynylene-substituted terpy ligand. Because this ligand is

(31) Boyarkin, O. V.; Rizzo, T. R.; Perry, D. S. *J. Chem. Phys.* **1999**, *110*, 11346, 11359.

(32) Islam, A.; Ikeda, N.; Nozaki, K.; Ohno, T. *Chem. Phys. Lett.* **1996**, *263*, 209.

(33) Islam, A.; Ikeda, N.; Yoshimura, A.; Ohno, T. *Inorg. Chem.* **1998**, *37*, 3093.

(34) Thompson, D. W.; Wishart, J. F.; Brunscwig, B. S.; Sutin, N. *J. Phys. Chem. A* **2001**, *105*, 8117.

(35) (a) Murtaza, Z.; Zipp, A. P.; Worl, L. A.; Graff, D. K.; Jones, W. E., Jr.; Bates, W. D.; Meyer, T. J. *J. Am. Chem. Soc.* **1991**, *113*, 5113. (b) Murtaza, Z.; Graff, D. K.; Zipp, A. P.; Worl, L. A.; Jones, W. E., Jr.; Bates, W. D.; Meyer, T. J. *J. Phys. Chem.* **1994**, *98*, 10504.

(36) (a) Coropceanu, V.; Malagoli, M.; da Silva Filho, D. A.; Gruhn, N. E.; Bill, T. G.; Bredas, J. L. *Phys. Rev. Lett.* **2002**, *89*, 275503. (b) Cometta, A.; Zucchelli, G.; Karapetyan, N. V.; Engelmann, E.; Garlaschi, F. M.; Jennings, R. C. *Biophys. J.* **2000**, *79*, 3235.

(37) (a) Chen, P.; Meyer, T. J. *Inorg. Chem.* **1996**, *35*, 5520. (b) Marcus, R. A. *J. Phys. Chem.* **1990**, *94*, 4963. (c) Barqawi, K. R.; Murtaza, Z.; Meyer, T. J. *J. Phys. Chem.* **1991**, *95*, 47.

(38) Balhausen, C. J. *Molecular Electronic Structures of Transition Metal Complexes*; McGraw-Hill: New York, 1979.

(39) (a) Lax, M. *J. Chem. Phys.* **1952**, *20*, 1752. (b) Lax, M.; Burstein, E. *Phys. Rev.* **1955**, *100*, 592.

(40) Strickler, S. J.; Berg, R. A. *J. Chem. Phys.* **1962**, *37*, 814.

(41) Cortes, J.; Heitele, H.; Jortner, J. *J. Phys. Chem.* **1994**, *98*, 2527.

(42) Chynwat, V.; Frank, H. A. *Chem. Phys.* **1995**, *194*, 237.

easier to reduce than is the terpy ligand in the parent complex, we would expect to observe a lower triplet energy for **1**. The weighted-average, medium-frequency vibrational mode coupled to nonradiative decay remains in the 1300–1400 cm^{-1} for both compounds, and the Huang–Rhys factors, S 's, are similar.

The rate constants, k_1 's, for nonradiative deactivation of the upper-lying excited triplet MLCT state are comparable for the two compounds, but the barrier height (E_A) is larger for **1**. It is interesting to note that the difference in barrier heights ($\Delta E_A = 275 \text{ cm}^{-1}$) is significantly smaller than the difference in triplet energies ($\Delta E_T = 1410 \text{ cm}^{-1}$). This suggests that the ethynylene substituent also lowers the energy of the upper-lying triplet state, and in turn, this is taken as an indication that the upper state possesses considerable MLCT character. Given the small barrier height, it is reasonable to suppose that barrier crossing is reversible.⁴³

The ethynylene substituent causes a marked increase in the activation energy for reaching the uppermost triplet state. On the basis of literature precedents,^{5,25,26} it seems likely that this high-energy state is of MC character. According to Figure 5, we associate this activation energy with charge transfer from the MLCT triplet to the metal center, thereby forming the MC state. For the parent complex, the energy gap between the lowest-energy MLCT triplet and the MC state has been calculated²⁶ to be ca. 1235 cm^{-1} . Because electron transfer is weakly endoergonic, it is likely to fall within the Marcus normal region so that the activation energy can be related to the accompanying reorganization energy (λ_{id}) and the energy gap (E_{TT}).⁴⁴ This leads to estimation of

$$E_B = \frac{(E_{\text{TT}} + \lambda_{\text{id}})^2}{4\lambda_{\text{id}}} \quad (8)$$

the reorganization energy as being ca. 3930 cm^{-1} . It has been reported⁴⁵ that λ_{id} for a somewhat related rhodium(III) complex is ca. 6400 cm^{-1} while that for the parent complex in the solid state³³ is ca. 5400 cm^{-1} . The increased barrier height found for **1** requires that either the reorganization energy is reduced or the energy gap is increased. Assuming the ethynylene substituent does not affect the reorganization energy for reaching the MC state, the energy gap for **1** will increase to 2555 cm^{-1} . This value compares well with the

energy gap ($E_{\text{TT}} = 2645 \text{ cm}^{-1}$) obtained by retaining the MC energy calculated for the parent complex²⁶ and using the triplet energy derived for **1**. Thus, the ethynylene substituent appears to have only a modest effect on the properties of the MC state. The more important effect is on the triplet energy of the MLCT states.

The radiative rate constant for the lowest-energy MLCT triplet, k_{RAD} , is significantly smaller for **1** than for the parent complex (Table 1), despite the larger transition moment. This is a consequence of the change in emission energy. It is possible that the derived M values reflect the relative singlet character associated with the radiative process. The radiative probability also depends on the energy gap between the emitting species and the perturbing singlet state.⁴⁶ This energy gap might, in part, refer to coupling to the upper triplet, and as such, we would expect a faster rate for the parent complex.

After allowing for the variation in triplet energy, and ignoring the various activated processes, it is clear that the triplet state of **1** is much longer lived. This effect can be traced to changes in the electron-vibrational coupling element, C , which for the parent complex is increased by a factor of 2. Although there are minor variations in the other parameters, it is this disparity in C that accounts for the different triplet lifetimes found at low temperature. It is notable that the Huang–Rhys factor remains similar for the two compounds. This latter term is related to the mean displacement and to the number of degenerate vibrational modes coupled to nonradiative decay. Because we lack vibrational spectroscopic data, it is not possible to examine if the invariance of S is a coincidence. However, it seems clear that the main effect of the ethynylene substituent is to reduce electron-vibrational coupling. Following the classical arguments of Weisman,⁴⁷ the relevant matrix element contains contributions from both vibronic and spin–orbit coupling processes.⁴⁶ It is not possible to separate these aspects at the present time, but ongoing Stark-effect spectroscopic studies might help resolve the finer details.

Acknowledgment. This work was supported by the EPSRC (GR/23305/01) and by the University of Newcastle. We would also like to thank the EPSRC-supported Mass Spectrometry Service at Swansea (U.K.) for running the ES-MS spectra. The laser flash photolysis studies were made at the FRRF housed at the Daresbury Laboratory.

IC035380E

(43) Juris, A.; Balzani, V.; Barigelletti, F.; Campagna, S.; Belser, P.; von Zewelsky, A. *Coord. Chem. Rev.* **1988**, *84*, 85.

(44) Marcus, R. A. *Annu. Rev. Phys. Chem.* **1964**, *15*, 155.

(45) Islam, A.; Ikeda, N.; Nozaki, K.; Ohno, T. *J. Photochem. Photobiol., A* **1997**, *106*, 61.

(46) McGlynn, S. P.; Azumi, T.; Kinoshita, M. *Molecular Spectroscopy of the Triplet State*; Prentice-Hall: Englewood Cliffs, NJ, 1969.

(47) Weisman, S. I. *J. Chem. Phys.* **1950**, *18*, 232, 1258.